



PAPER • OPEN ACCESS

Analysis of the thermal properties in short sansevieria cylindrica fibre/PLA composites processed by twin screw extruder followed by hot press molding technique

To cite this article: Senthilkumar Krishnasamy *et al* 2024 *Mater. Res. Express* 11 035506

View the [article online](#) for updates and enhancements.

You may also like

- [Physical and mechanical properties of natural fiber from *Sansevieria trifasciata* and *Agave sisalana*](#)
A Widyasanti, L O B Napitupulu and A Thoriq
- [Thermal degradation and tensile strength of sansevieria trifasciata-polypropylene composites](#)
H Abrial and E Kenedy
- [Effects of fiber loadings and lengths on mechanical properties of *Sansevieria Cylindrica* fiber reinforced natural rubber biocomposites](#)
Sivasubramanian Palanisamy, Mayandi Kalimuthu, Shanmugam Dharmalingam *et al.*

The Breath Biopsy® Guide
Fourth edition

FREE

DOWNLOAD THE FREE E-BOOK

BREATH BIOPSY

OWLSTONE MEDICAL

Materials Research Express



PAPER

OPEN ACCESS

RECEIVED
17 January 2024

REVISED
27 February 2024

ACCEPTED FOR PUBLICATION
12 March 2024

PUBLISHED
3 April 2024

Original content from this work may be used under the terms of the [Creative Commons Attribution 4.0 licence](#).

Any further distribution of this work must maintain attribution to the author(s) and the title of the work, journal citation and DOI.



Analysis of the thermal properties in short sansevieria cylindrica fibre/PLA composites processed by twin screw extruder followed by hot press molding technique

Senthilkumar Krishnasamy¹ , Thitinun Ungtrakul², M Chandrasekar³ , T Senthil Muthu Kumar^{4,9,10} , Jyotishkumar Parameswaranpillai⁵ , H Mohit⁶, D Aravind⁷ , N Rajini⁴ , Suchart Siengchin² and Varagunapandiyan Natarajan⁸

¹ Department of Mechanical Engineering, PSG Institute of Technology and Applied Research, Coimbatore—641062, Tamil Nadu, India

² Department of Materials and Production Engineering, The Sirindhorn International Thai-German Graduate School of Engineering (TGGS), King Mongkut's University of Technology North Bangkok, Bangkok, Thailand

³ Simcrash Centre, Department of Aerospace Engineering, Hindustan Institute of Technology & Science, Padur, Kelambakkam, Chennai—603103, Tamil Nadu, India

⁴ Department of Mechanical Engineering, Kalasalingam Academy of Research and Education, Krishnankoil—626126, Tamil Nadu, India

⁵ Department of Science, Faculty of Science & Technology, Alliance University, Bengaluru—562106, India

⁶ Department of Mechanical Engineering, Alliance College of Engineering and Design, Alliance University, Bengaluru—562106, India

⁷ University Science Instrumentation Centre, Madurai Kamaraj University, Palkalai Nagar, Madurai—625021, Tamil Nadu, India

⁸ Department of Chemical Engineering, King Khalid University, Abha, Saudi Arabia

⁹ Department of Mechanical Engineering, INTI International University, Persiaran Perdana BBN, Putra Nilai, 71800 Nilai, Negeri Sembilan, Malaysia

¹⁰ Centre for Advanced Composite Materials (CACM) Universiti Teknologi Malaysia, 81310 Skudai, Johor Bahru, Johor, Malaysia

E-mail: kmsenthilkumar@gmail.com

Keywords: short Sansevieria cylindrica fibre, polylactic acid, biocomposites, twin screw extruder, hot press moulding, thermal properties

Abstract

Short Sansevieria cylindrica fibre/poly(lactic acid) composites (SCFP) were fabricated using a twin screw extruder followed by the hot press technique, with variations in fibre loadings of 10 wt%, 20 wt%, 30 wt% and 40 wt%. The thermal properties of SCFP were assessed through dynamic mechanical analysis (DMA), thermomechanical analysis (TMA), thermogravimetric analysis (TGA) and differential scanning calorimetry (DSC). Notably, the samples loaded with 40 wt% of fibre exhibited an increased storage modulus. In terms of loss modulus, the fibre-loaded samples displayed high values, indicating more heat is released during DMA experiment. Interestingly, the composite trend did not solely rely on increasing fibre loading, highlighting the intricate interplay between reinforcement and matrix crucial for determining viscoelastic properties across various temperatures. The TGA results revealed a decrease in inflection temperature with increasing fibre loadings, accompanied by a proportional rise in residues. The DSC thermograms indicated minimal differences in T_g , T_{cc} , and T_m values among composites with varying fibre loadings. However, neat PLA showed slightly higher values than the composites. On the other hand, reinforcing SCF into the PLA matrix promoted the crystallization of PLA by 1%–3% with the maximum degree of crystallinity of 25.4% obtained for 30 wt% of SCFP.

1. Introduction

In recent years, the demand for environmentally friendly products in all fields has increased rapidly because of the increased awareness of their benefits. As a result, biobased materials have become more common in the composite industry [1]. Furthermore, researchers and manufacturers place the utmost importance on renewable and biodegradable materials to protect the environment and people's health in every possible way. Many industries, including aerospace, automotive, marine, food packaging, electronics, and transportation, are keen to utilise cellulose-based products in various applications [2].

Cellulose-based composites offer numerous advantages, including low density, cost-effectiveness, environmentally friendliness, good specific properties, ease of processing, and non-abrasiveness. Moreover, natural fillers-based reinforcements allow the ability to harness local resources in less industrialized countries, thereby improving materials and technologies while considering environmental impact [3].

Many authors have reported using natural fibres as reinforcements in thermoplastic matrices [4]. Thermoplastics offer several advantages when used with natural fibres, including ease of processing (as thermoplastics can be melted and re-melted), better adhesion, low energy consumption, recyclability, ductility, and impact resistance [5]. Additionally, many thermoplastic polymers that possess high thermal resistance have been developed. Thus, they are interested in the use of aerospace applications [6].

In this paper, short *Sansevieria cylindrica* fibres (SCF) were utilized as reinforcements in a PLA matrix. Fibrous plants are plentiful in tropical countries, and *Sansevieria cylindrica*, a wild plant native to Africa and Asia, belongs to the Asparagaceae family. Numerous researchers [7–9] have explored their applications in various fields. According to their findings, the extraction and processing of these fibres are straightforward, making them a commonly recommended choice for reinforcing lightweight materials.

Yu *et al* [10] investigated the linear coefficients of thermal expansion behaviour in various wheat straw/PP composites, ranging from 20 wt% to 65 wt%. The experiments were conducted at 20 °C to –13 °C and –13 °C to 60 °C. The results reported that increased wheat straw content contributed to a reduction in thermal expansion behaviour. For instance, samples loaded with 65 wt% wheat fibre exhibited ~70% decrease in thermal expansion compared to those with 20 wt% wheat fibre. This result was ascribed to the capability of the reinforcement to restrict the deformation of PP molecular chains and hinder the flow of the plastic matrix. Zabihzadeh [11] investigated the thermal properties of wheat straw flour reinforced with high-density polyethylene (HDPE) and PP matrices. The study revealed that the type of matrix materials and the interfacial bonding between reinforcements and matrix materials significantly influenced the thermal properties. Moreover, the wheat straw/PP composites displayed lower thermal stability than the wheat straw/HDPE composites. Additionally, introducing maleic anhydride polypropylene (MAPP) and maleic anhydride polyethylene (mAPE) improved the results by enhancing the adhesion between wheat straw flour and matrix materials, consequently increasing thermal stability.

Yang *et al* [12] investigated the DSC and DMA behavior of natural fillers (rice husk and wood flour) reinforced with PP matrix. The DSC results indicated a notable influence of the addition of MAPP on the T_g of the composites, attributed to the enhanced chemical bonding between the fillers and the matrix. However, the melting temperature of the composites remained unaffected by the presence of fillers. In the context of DMA, the storage modulus of biocomposites showed enhancements compared to the PP matrix. This improvement was observed as the fillers facilitated the transfer of stresses across the reinforcement to the matrix. Yılmaz and Akar [13] examined the TGA and differential thermal analysis of short rape fibres reinforced with three different matrices, namely HDPE, polystyrene and polyoxymethylene. The results showed that the rape reinforcement element burned before the matrix materials, resulting in a delayed burning process in thermoplastics. As a consequence, the rape-reinforced HDPE composites showed improvements in mechanical characteristics. Azammi *et al* [14] fabricated thermoplastic composites by varying the mixtures of kenaf fibre, natural rubber and thermoplastic polyurethane while maintaining a total weight of 40 g in each composite. The results reported that the natural rubber content in the composites influenced the overall weight loss and char residue. For instance, increased natural rubber content in the composites resulted in higher weight loss. Jumaidin *et al* [15] examined the impact of durian peel fibre/thermoplastic cassava starch composites on their thermal characteristics. The results revealed that the thermal behaviour of composites exhibited an increase, as observed by higher onset decomposition temperatures. Adding durian peel fibres contributed to an enhanced biodegradation rate, making the materials more environmentally friendly. Besides, the 40 wt% of durian peel fibre composites showed superior performance compared to other fibre-loaded samples. In another study, Ming *et al* [16] studied the effect of ternary composites of polybutylene adipate terephthalate/thermoplastic cassava starch/lignin. The results reported that adding lignin increased thermal stability and T_g was also improved. This was evident in the increased thermal resistance of the composite materials. Besides, the lignin enhanced the interfacial compatibility between the polybutylene adipate terephthalate/thermoplastic cassava starch. Hafila *et al* [17] explored the thermal behavior of thermoplastic cassava starch containing palm wax by varying its ratios from 2.5 wt% to 15 wt%. The TGA results showed that the thermal stability of thermoplastic cassava starch increased as the palm wax content increased.

Based on the extensive review of the existing literature survey, it was evident that no prior research had explored the thermal characteristics of SCFP. Considering this gap, the primary objective of this study was to investigate the impact of varying short SCF loadings: 10 wt%, 20 wt%, 30 wt% and 40 wt% on thermal characteristics of biocomposites. The fabrication of these composites is made by using a twin-screw extruder followed by hot press techniques. A comprehensive set of analyses was carried out to investigate the thermal behavior of these fabricated composites, encompassing dynamic mechanical analysis, thermomechanical

Table 1. Chemical and physical properties of SCF [18].

Cellulose (%)	Hemicelluloses (%)	Lignin (%)	Wax (%)	Moisture (%)	Density (g/cm ³)
79.7	10.13	3.8	0.09	6.08	0.915

Table 2. PLA properties.

Tensile yield strength (MPa)	Tensile modulus (GPa)	Elongation at break (%)	MFI (g/10 min) (2.16 kg, 210 °C)	Specific gravity (g/cc)
60	3.6	6.0	6	1.24

analysis, thermogravimetric analysis, and differential scanning calorimetry. In conclusion, the short SCFP, exhibiting improved thermal characteristics, hold promise for applications as biodegradable materials.

2. Experimental

2.1. Materials

SCF was collected from local sources in Hyderabad, India, while the matrix, polylactic acid (PLA) (grade INGENO 4043D) was purchased from Nature Friend Company Limited, Thailand. The essential properties of SCF and PLA are provided in tables 1 and 2.

2.2. Comparative analysis of fibre-reinforced composites

Table 3 compares the DMA, TGA, and DSC properties of composite materials with varying fibre lengths and loadings.

These observations showed that fibre length, fibre content, and fibre size significantly influence the thermal behavior of fibre-reinforced composites. Additionally, it was observed that optimum values or configurations vary for specific composite materials and their intended applications. Hence, it was decided to use micron-sized fibres ranging from 10 to 30 microns and lengths from 50 to 200 microns for examining the thermal behavior of SCFP by varying the fibre loadings from 10 wt% to 40 wt%. The details of composite fabrication are given below.

2.3. Fabrication of SCFP

Initially the SCFs were cut into micron-sized lengths using a specialized fibre micro-cutting machine (Universal cutting mill, Branch - Fritsch, Model—Pulverisette 19). The fibres used in the fabrication process appeared to have diameters ranging from 10 to 30 microns and lengths from 50 to 200 microns, which are typical for micron-sized fibres used to reinforce polymer matrices. The fine micron-sized fibres were blended with a PLA matrix using a high-speed mixing machine (Unique tools, Model: 5L). Once the mixtures of fibres and PLA were prepared, they were carefully deposited into the hopper of a twin-screw extruder machine (XINDA, PSHJ-20) for the purpose of thorough blending. Detailed barrel temperature settings, including those for the feed zone, compression zone, melting zone, and die, can be found in table 4 for reference.

The resulting blend of fibre and matrix was then extruded into uniform mixtures, which were precisely cut using a strand pelletizer. A similar procedure was followed to produce filament extrusion ratios of 10 wt%, 20 wt%, 30 wt% and 40 wt% of SCFP. Before being introduced to the hot press machine, all the extruded mixtures were pre-heated in a hot air oven to remove moisture that may be presented in the fabricated samples. In the hot press molding machine, a temperature of 170 °C was maintained, with a pressure of approximately 2000 psi applied for 10 min. Following the molding process, the fabricated samples were left in a hot air oven at a temperature of 60 °C for 24 h for moisture removal. This step may help in improving the properties. Table 5 gives the details of fabricated samples. Subsequently, the samples underwent thermal tests to assess their performance. Table 6 gives the step-by-step procedure of composite fabrication.

2.4. Characterization of SCFP

2.4.1. Dynamic mechanical analysis (DMA)

The SCFP were subjected using DMA to investigate their viscoelastic behavior following ASTM D5418 [24]. The DMA/SDTA861^e instrument from Mettler Toledo was used. The testing was carried out within ranges of 20 °C to 120 °C, maintaining a constant frequency of 1 Hz with a temperature ramp rate of 3 °C min⁻¹. Testing

Table 3. Comparative study analysis on thermal properties of composites.

Type of reinforcement	Fibre dimensions varied	Property examined	Significant observations	References
Banana stem, pineapple leaf, S-glass fibres and Epoxy resin	Fibre lengths varied: 20 cm, 30 cm and 40 cm	DMA	<ul style="list-style-type: none"> An increase in fibre volume fraction and length helped enhance the thermal properties up to a fibre volume fraction of 40%. 	[19]
Wood flour, rice hulls, kenaf fibres, newsprint and polypropylene (PP)	Fibre volume fractions: 30%, 40% and 50% Fibre loading of 25% and 50% by weight	DMA	<ul style="list-style-type: none"> 40 cm fibre length was the optimum fibre length in storage modulus. Increasing the fibre loading in PP helped enhance the storage modulus of composites. The same behavior of observed in all natural fibres and fibre content. These results indicate that the stiffness of the fibre-reinforced composites improved while the damping values were decreased. 	[20]
Hemp fibre/PP/ poly(styrene-b-(ethylene-co-butylene)-b-styrene) (SEBS)	Fibre length ranged from 1 mm to 4 mm	TGA, DMA, DSC	<ul style="list-style-type: none"> The longer fibre-reinforced composites exhibited higher crystallinity. Increased stiffness was correlated with improved crystallinity values. The storage modulus of composites increased by 82 to 90% using longer fibre-reinforced composites. Variations of fibre length influenced minor changes in composite degradation, and their temperature differences, such as first-step and second-step degradation temperatures, were less than 3 °C. DSC results showed that the length of the hemp fibre did not affect the melting temperature of composites. The crystallization temperature was decreased in composite samples. This was attributed to good fibre-matrix interfacial bonding. Besides, an increase in crystallinity was observed by increasing the fibre lengths. 	[21]
Wood flour, rice hulls, kenaf fibres, newsprint and high density polyethylene	Fibre loading of 25% and 50% by weight	TGA, DSC	<ul style="list-style-type: none"> Among the natural fibres, the kenaf fibres exhibited the least thermal stability, while the newsprint fibres showed improved thermal stability in the composites. Regarding the fibre loading, 50% of fibre-loaded samples exhibited faster degradation and higher weight loss than 25% of fibre-loaded samples. 	[22]
E glass/PP	Fibre sizes varied from 1mm to 0.3 mm, and different fibre loadings were 10 wt%, 15 wt%, 20 wt% and 30 wt%	DSC	<ul style="list-style-type: none"> The activation energy increased with increasing fibre loading. This activation energy was required for crystallization in the composites. These results indicate that more energy was required to initiate the crystallization process. 	[23]

Table 4. Setting of barrel temperatures.

Feed zone	Compression zone		Metering zone		Die
D1	D2	D3	D4	D5	
120 °C	145 °C	155 °C	165 °C	165 °C	160 °C

Screw speed: 500 rpm.

Table 5. Details of fabricated samples.

Abbreviations	Details of samples
PLA	Polylactic acid
SP 10	10 wt% of SCFP
SP 20	20 wt% of SCFP
SP 30	30 wt% of SCFP
SP 40	40 wt% of SCFP

samples had dimensions of $22 \times 13 \times 3 \text{ mm}^3$ (length \times width \times thickness) for dual cantilever mode. Storage modulus (E'), loss modulus (E'') and tan delta ($\tan \delta$) were determined for these fabricated samples.

2.4.2. Thermomechanical analysis (TMA)

TMA was performed in expansion mode using the Mettler Toledo (TMA/SDTA 2+ HT/1600) instrument, following ASTM E831 standards [25]. The temperature range maintained was 20 °C to 120 °C, with a ramping rate of 3 °C min⁻¹. The coefficient of linear thermal expansion was calculated using equation (1).

$$\alpha = \frac{1}{L_i} \left(\frac{\Delta L}{\Delta T} \right)_p \quad (1)$$

where,

α = Plot shows the dimensional changes against temperature variations, whereby the sample's expansion is linear within the temperature ranges ΔT at isobaric pressure 'p'.

ΔL = Dimensional change in the linear expansion region at temperature range ΔT and isobaric pressure 'p'.

L_i = Initial length of the fabricated composite sample.

2.4.3. Thermogravimetric analysis (TGA)

TGA measurements were conducted using a TGA/DSC 3+ thermogravimetric analyser (Mettler Toledo) with a 70 μl alumina ceramic holder following ASTM E1131 [26]. The measurements were performed under a nitrogen atmosphere with a gas flow rate of 50 ml min⁻¹, a scanning rate of 10 °C min⁻¹, and a temperature of 25 °C to 600 °C. The mass of each sample ranged from 15 to 20 mg was used.

2.4.4. Differential scanning calorimetry (DSC)

The DSC Q2000 from TA instruments were employed to examine the DSC study of PLA and its composite samples using a 40 μl aluminium holder. The test was conducted according to ASTM D5418 [27] under a nitrogen atmosphere with a gas flow rate of 50 ml min⁻¹. During testing, the samples were subjected to temperature ranges between 0 °C to 240 °C at a rate of 10 °C min⁻¹. The mass of each sample ranged from 15 to 20 mg was used.

3. Results and discussion

3.1. Dynamic mechanical analysis (DMA)

The DMA of short SCFP was examined to investigate their viscoelastic behaviour as a function of temperature. During testing E' , E'' and $\tan \delta$ were obtained by varying time and frequency. E' gives the composites' stiffness or elasticity and exhibits how the composites' rigidity varies with respect to temperature. Moreover, it reveals elastic behavior by showcasing the energy stored in a viscoelastic material. This property is crucial for evaluating the suitability of composites for diverse applications [28, 29].

Figure 1 shows the E' of pure PLA and various fibre-loaded composite samples, with temperatures ranging from 20 °C to 120 °C. Notably, it was evident that the E' of all the samples decreased as the temperature increased. This behaviour was ascribed to the softening effect of the matrix [30]. PLA shows a relatively higher E'

Table 6. Step-by-step procedure of composite fabrication.

Steps involved	Details of composite fabrication
	Universal cutting mill used to cut the SCFs
	Chopped fibres
	SCFs were mixed with PLA matrix using a high-speed mixing machine (Unique tools, Model: 5L)





Table 6. (Continued.)

Steps involved	Details of composite fabrication
	PLA samples were deposited in hopper of twin-screw extruder
	The PLA samples were moved to the next stage in twin-screw extruder
	The PLA was melted using twin screw extruder and extruded filaments were formed

Table 6. (Continued.)

Steps involved	Details of composite fabrication
	The extruded PLA filaments
	The extruded filaments of SCF/PLA
	Different fibre loaded samples such as 10 wt%, 20 wt%, 30 wt% and 40 wt% and neat PLA

Table 6. (Continued.)

Steps involved	Details of composite fabrication
	PLA was deposited over the mold
	The PLA was filled in mold and loaded in hot press moulding machine at 170 °C for 10 min
 	Fabricated samples

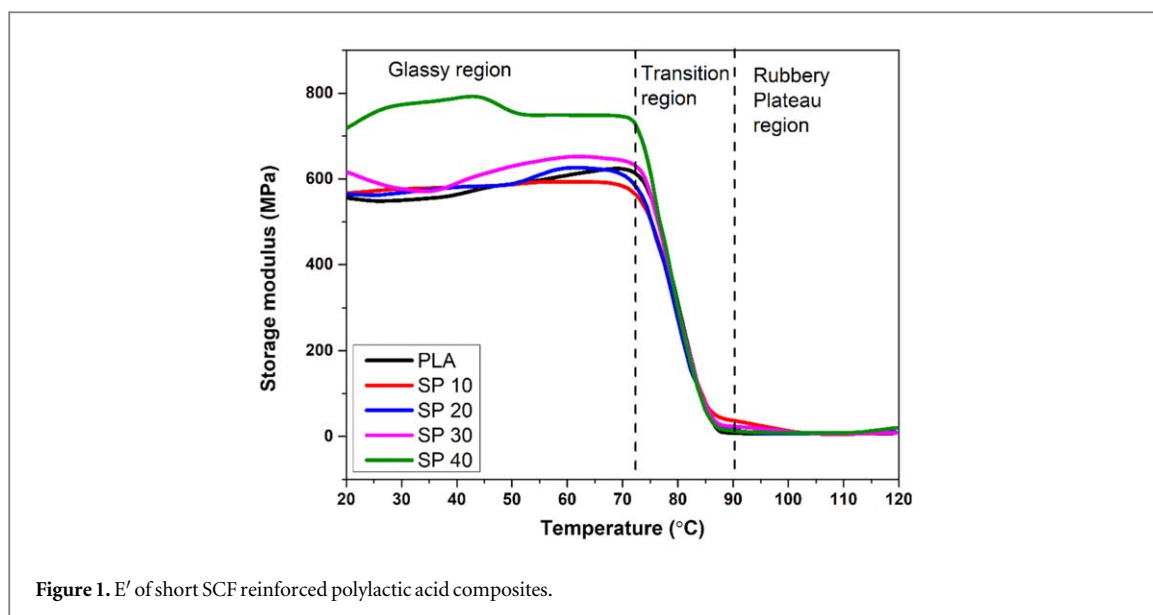


Figure 1. E' of short SCF reinforced polylactic acid composites.

(~555MPa) at the lowest temperatures ranging from 20 °C to 25 °C (figure 1). This modulus value indicated that PLA was in a glassy state and in a rigid phase. In the glassy region, the relatively immobile polymer chains also exhibited solid-state behaviour [2]. As the temperature increased, there was a decrease in the E' due to the transition from a glassy region to a rubbery region at above >72°. This glass transition made the PLA chains more mobile, reducing stiffness [31, 32]. When the temperature was >118 °C, PLA's E' continuously decreased, indicating that the PLA became more flexible and the E' reached a very low value (~7MPa). During this stage, the segmental mobility of polymers further increased, or polymer chains even start to flow, and PLA exhibited a more significant loss of rigidity. 20 wt% of fibre-loaded composite samples (i.e., 20 SP) consistently exhibited higher E' than PLA samples due to the reinforcing effect of short SCFs. The composites showed improved stiffness and rigidity at lower temperature ranges [33]. When the temperature was within the glass transition ranges, the 20 SP showed a greater E' than PLA, because the fibres helped enhance the material's temperature stability (the SP 20 sample exhibited a residue of 4.03%, in contrast to PLA's 1.41% (TGA studies)). This higher residue indicates improved thermal stability, likely attributed to the reinforcing effect. Refer table 10 for detailed data) and stiffness in the glass transition phase. When the temperature was increased, the SP 20 continued to show higher E' . This behaviour indicated that it remained stiffer and rigid in the rubbery region. The stiffer and rigidity in the glassy region is advantageous in various applications that require both flexibility and strength [34].

Accordingly, the SP 30 samples consistently showed a higher E' than PLA, SP 10 and SP 20. It was ascribed to increasing the fibre loading, which further enhanced the E' and rigidity of respective composite samples. The SP 30 outperformed in the glass transition regions, highlighting the reinforcing effect of fibres. Thus, the composite materials maintained better stiffness in the glass transition region. Even at higher temperatures, the SP 30 continued to exhibit a higher E' , emphasized to resist softening (more resistance in polymer mobility due to the presence of fibres) than pure PLA samples.

The SP 40 showed the highest E' throughout the temperature range. The higher fibre content increases the stiffness, making it the stiffest material among all the samples. The SP 40 also maintained a higher E' in glass transition and rubbery regions. Sreenivasan *et al* [35] examined the E' of SCF-reinforced polyester composite by varying fibre loadings from 10 wt% to 50 wt% (in increments of 10 wt%). Results reported that the 30 wt% of composite samples showed the highest E' due to their better interfacial bonding between fibre and matrix.

The E'' represents the ability of SCFP to dissipate energy as heat, primarily attributed to frictional forces caused by the fiber and polymer. Figure 2 depicts the variations in E'' with the temperature of various fiber-loaded composites. Notably, the pure PLA matrix displayed the lowest E'' value among the fabricated samples, owing to its limited heat dissipation capacity [36].

Furthermore, it was evident that the E'' of all the samples reached a peak value before decreasing as the temperature increased. This behavior was ascribed to increased molecular mobility within the polymer chains [28]. In the case of composites, as the fibre loading increased, the E'' also increased. Remarkably, at higher temperatures (>68 °C), the difference in E'' between the SP 10 and PLA became more pronounced. The composite exhibited a higher E'' , indicating that it retained its viscoelastic properties even at higher temperatures. However, a different trend emerged when fibre loading was increased in the PLA matrix.

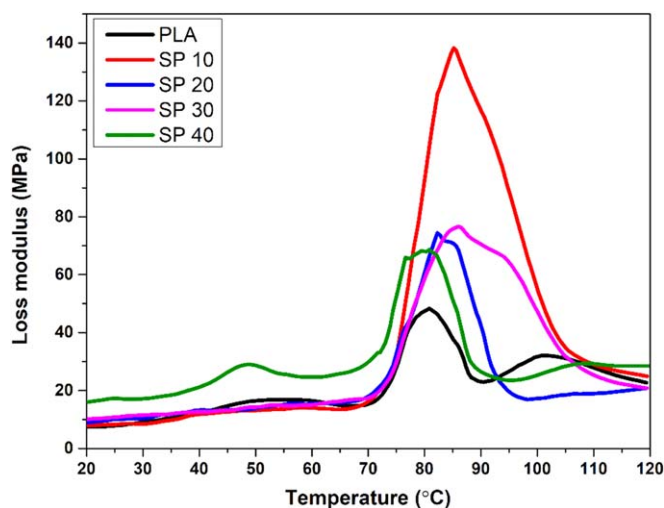


Figure 2. E'' of short SCF reinforced polylactic acid composites.

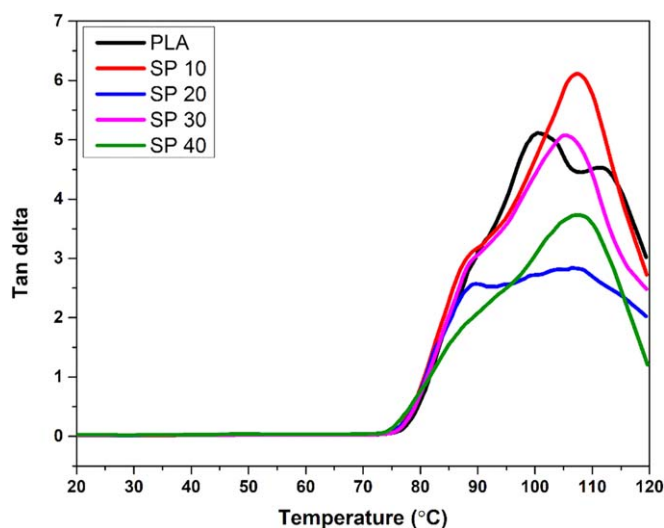


Figure 3. $\tan \delta$ of short SCF reinforced polylactic acid composites.

Table 7. Glass transition temperature of various SCFP.

Sample details	Glass transition temperature (T_g)
PLA	80.85 °C
SP 10	85.15 °C
SP 20	82.25 °C
SP 30	86.45 °C
SP 40	80.8 °C

Table 7 gives the T_g of various fibre-loaded samples. It is observed that T_g of composite samples increased in most cases by increasing the fibre loading.

$\tan \delta$ is a dimensionless quantity in DMA, representing a damping characteristic of a material. It is the ratio of E'' to E' , quantifying energy dissipation to stored energy. For instance, if the $\tan \delta$ value is higher, the material dissipates more energy as heat when subjected to stress. This characteristic is typical of a viscoelastic material in the rubbery region [28, 34]. Figure 3 illustrates the variation of $\tan \delta$ with temperature for neat PLA and various composites fabricated by incorporating short SCF. In the case of neat PLA, two relaxation peaks are observed in

Table 8. Tan δ and T_g of various SCFP.

Sample details	Tan δ peak height	T_g (°C)	Observations
PLA	5.109	100.85	
SP 10	6.117	107.35	<ul style="list-style-type: none"> • Higher tan δ—high damping property • T_g suggests—good thermal stability and resistance to deformation at elevated temperature
SP 20	2.840	106.35	<ul style="list-style-type: none"> • Lower tan δ value—reduced energy dissipation indicating a potentially a stiffer material • T_g suggests—good thermal stability
SP 30	5.075	105.45	<ul style="list-style-type: none"> • Increase in tan δ—enhancement in energy dissipation could be due to improved damping property • T_g indicates a good thermal stability
SP 40	3.728	107.05	<ul style="list-style-type: none"> • Decrease in tan δ value—trend towards a stiffer material • T_g indicates—good thermal stability

the tan δ curves. The primary relaxation peak curve occurred at a temperature of around 100 °C, which can be attributed to the T_g of PLA. This peak marked the point at which the PLA transformed from a glassy, brittle state to a more flexible, rubbery state due to the increased molecular mobility of the PLA. Additionally, a 2nd transition was observed in figure 3, occurring around 117 °C. This observation was ascribed to changes in the movement of polymer chains within the crystalline region. These changes indicate the complex thermal characteristics of the material [35].

Table 8 shows the peak value of tan δ , glass transition temperature, and significant observations of neat PLA and its composite samples. For example, the T_g of pure PLA sample is 100.85 °C. With an increase in SCFs within the PLA matrix, the T_g of each composite sample increased and shifted towards higher temperatures. This shift towards higher temperatures is ascribed to the improved effectiveness of fibre reinforcement in PLA [37].

Additionally, the tan δ values were observed to decrease, possibly due to the improved interfacial bonding characteristics of fibre to the matrix. A decrease in tan δ values suggested enhanced interfacial bonding. Conversely, higher tan δ values at the interfaces indicated poorer interface adhesion, highlighting the significance of interfacial interactions in composite materials [38, 39].

3.2. Thermomechanical analysis (TMA)

Figures 4(a), (b) depict the thermal expansion behavior of both neat PLA and composites reinforced with short *Sansevieria cylindrica* fibers. Thermal expansion refers to the material's dimensional change in response to temperature variations. The thermal expansion is reduced with the addition of fibers, this behavior is attributed to the interfacial adhesion properties between the fibers and matrix in composite materials. The enhanced interfacial properties reduce thermal expansion, suggesting less dimensional change [40].

Figure 4(a) reveals that the neat PLA matrix exhibited a more pronounced dimensional change as the temperature increased from 25 °C to 120 °C. Because the molecular chains within the polymer was moved vigorously with higher thermal energy, caused the material to expand. Consequently, the PLA matrix expanded, leading to an increase in its overall dimensions [41].

In contrast to this behaviour, the thermal expansion of composites reinforced with short SCFs was decreased, particularly in the case of SP 20. This observation can be ascribed to the restraining effect imposed on thermal expansion by the short SCFs [42].

In alignment with this observation, figure 3 shows that the SP 20 exhibited a low tan δ value (2.840). This value implied that the material is relatively stiff and has good elastic properties. Furthermore, composites characterized by low tan δ values typically exhibit increased resistance to deformation and damping when subjected to dynamic loads. In the context of thermal expansion behaviour, materials with low tan δ values are expected to give lower thermal expansion. Because they are less likely to deform or expand under temperature changes. They tend to retain their shape and dimensions, showing a more elastic response to temperature changes. Hence, the SP 20 exhibited the least thermal expansion compared to other samples due to their good interfacial properties and elastic behaviour, as reflected in their tan δ values. Figure 4(b) and table 9 show the coefficient of thermal expansion of PLA and its composite samples. It was evident that among the fabricated samples, SP 20 showed the lowest thermal expansion behavior at elevated temperatures. A lower CTE is preferable for materials in a wide range of applications where dimensional stability is critical, such as electronics and precision engineering.

3.3. Thermogravimetric analysis (TGA)

TGA is used to examine the thermal stability of polymers by monitoring the weight change of a polymer since the polymer is heated at a constant rate [43]. This analysis provides data on thermal degradation. For instance, at

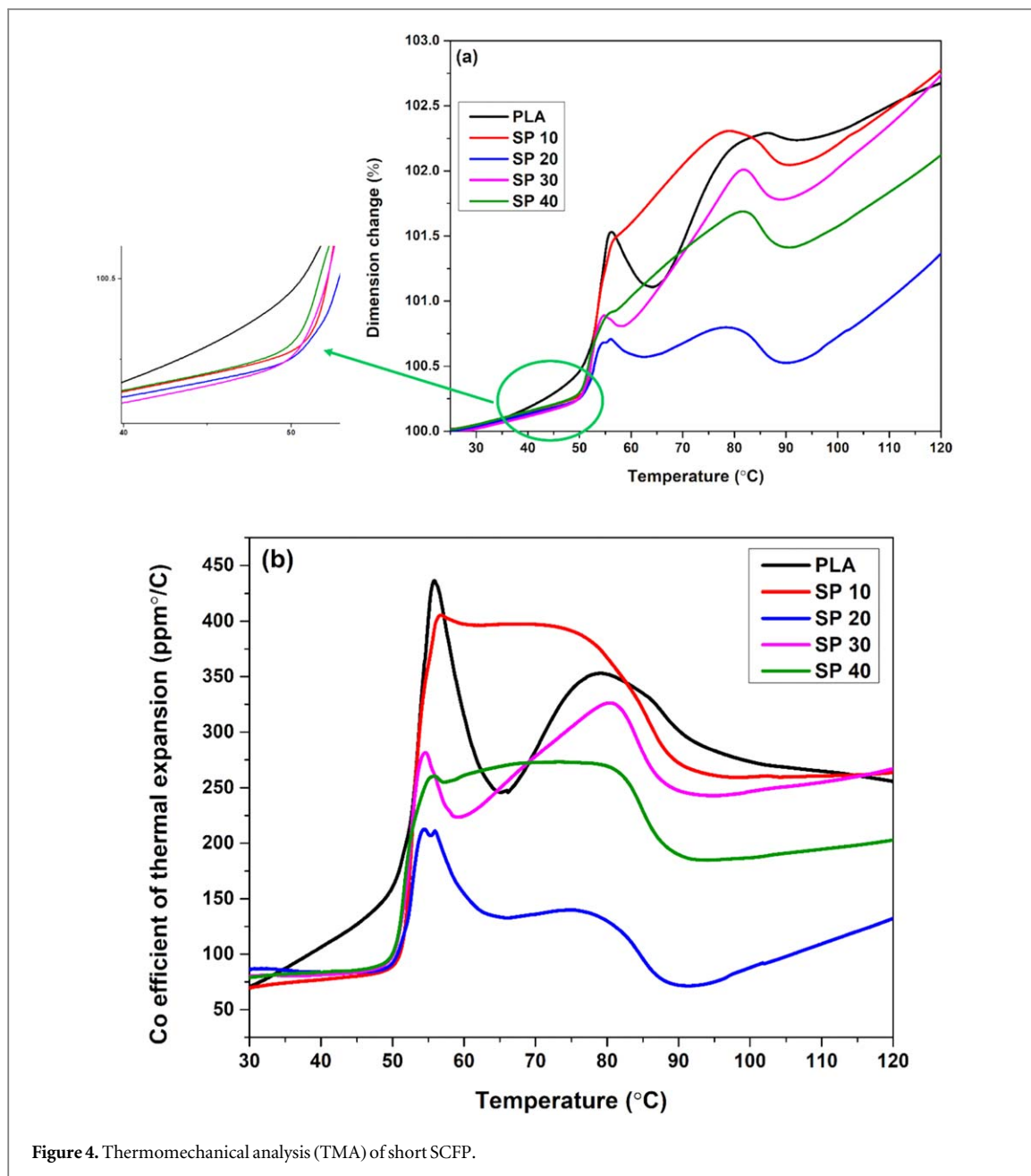


Figure 4. Thermomechanical analysis (TMA) of short SCFP.

Table 9. Coefficient of thermal expansion of PLA and various SCFP.

Temperature (°C)	Coefficient of thermal expansion (ppm/°C)				
	PLA	SP 10	SP 20	SP 30	SP 40
40	106.15	76.92	83.66	81.35	83.61
50	160.29	89.17	91.95	98.8	100.36
60	315.07	397.58	154.58	224.48	261.09
70	283.56	397.13	136.02	278.26	272.69
80	352.15	367.3	130	326.17	269.4
90	301.74	272.27	72.02	247.38	189.66
100	273.45	259.66	87.8	246.51	186.81
110	264.83	260.54	109.17	254.8	194.47
120	255.58	263.66	132.29	267.03	202.86

what temperature the PLA and its composites start to decompose, rates of decomposition, etc The thermal stability of examined polymers and their composites is significant in determining the performance of PLA and composites for their intended applications. For instance, a material that has higher thermal stability may be

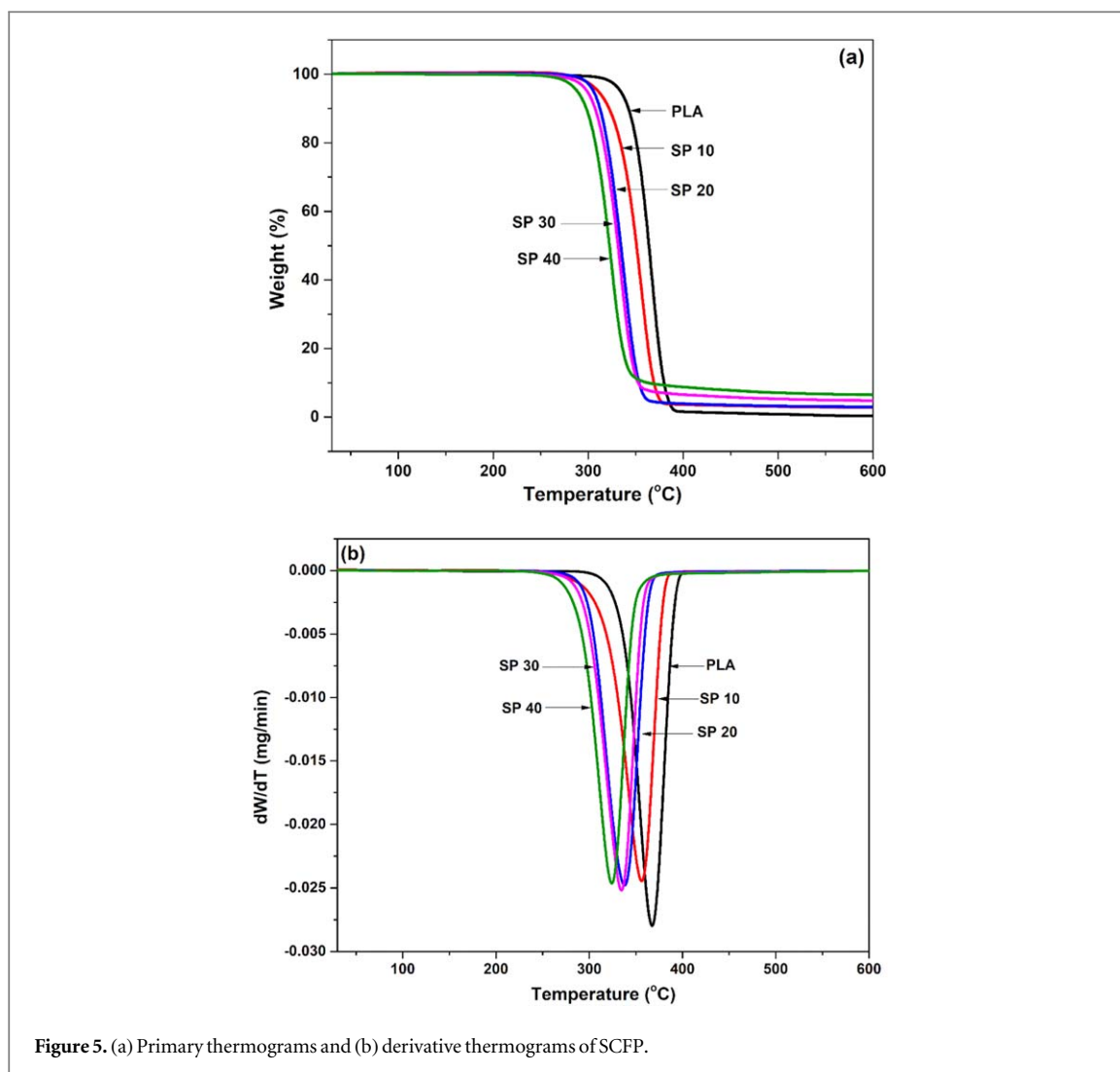


Figure 5. (a) Primary thermograms and (b) derivative thermograms of SCFP.

Table 10. Thermal properties of SCFP.

Samples	Onset temperature (°C)	Inflection temperature (°C)	Endset temperature (°C)	Residue (%)
PLA	339.1	360.0	372.3	1.41
SP 10	322.8	348.8	360.7	3.69
SP 20	307.0	330.7	344.2	4.03
SP 30	304.9	327.5	339.3	6.91
SP 40	295.6	317.0	329.9	9.01

suitable for high-temperature applications without experiencing major degradation [44]. The thermal stability of the SCFP was assessed through thermogravimetric analysis, and the thermograms depicting the temperature-dependent behavior of neat PLA and its composites with varying wt% of SCFP are presented in figure 5.

Generally, the mass loss occurs in two or three stages depending upon the composite's fibre composition, such as removing the absorbed moisture, hemicellulose, lignin and cellulose components, and finally, the depolymerization of the matrix material [45]. It is clearly evident from the primary and derivative thermograms that the decomposition temperature of the composites shifted to the lower side with an increase in the fibre contents. Increased fibre loading in composites can result in a significant rise in water molecules. The disintegration of molecules at the intermediate mass loss zone (between 200 °C and 400 °C) weakens the interface, accelerating composite breakdown [46]. The thermal properties of PLA and its composites are presented in table 10. Table 10 shows that the inflection temperature decreases with increased fibre contents, whereas the residues increase with increasing fibre contents. This indicates the severe occurrence of coking and carbonization [46].

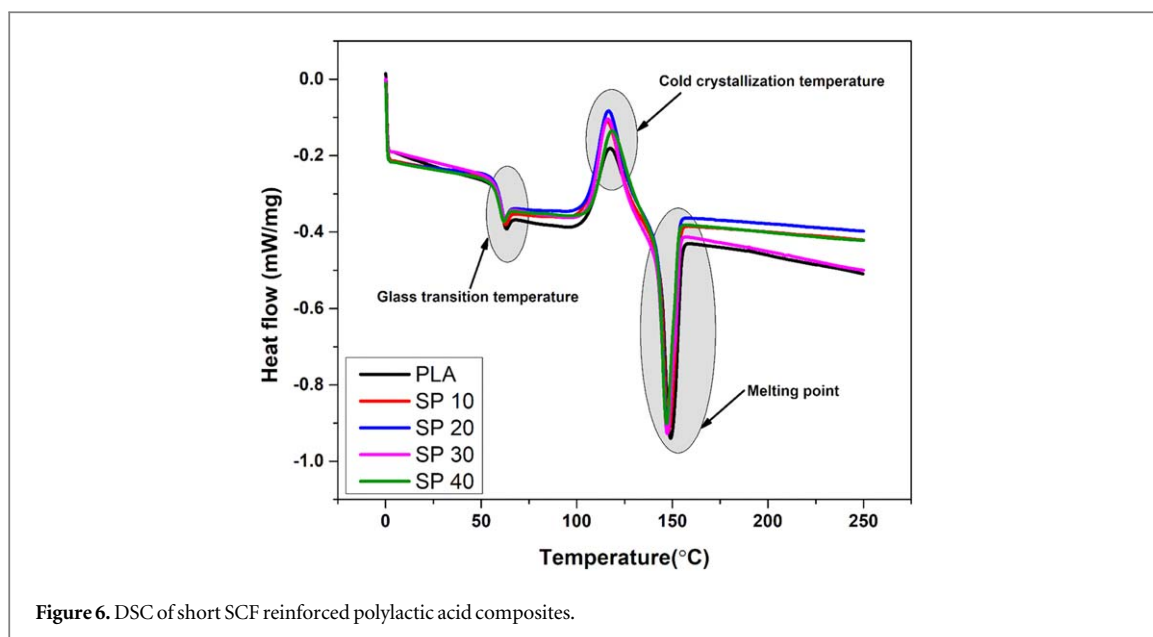


Figure 6. DSC of short SCF reinforced polylactic acid composites.

Table 11. DSC results of SCFP.

Samples	T_g (°C)	T_{cc} (°C)	T_m (°C)	ΔH_f	X_c (%)
PLA	60.44	117.83	149.50	21.68	22.8
SP10	59.89	116.17	148.17	23.14	24.5
SP20	59.34	116.67	147.50	22.35	23.5
SP30	59.49	116.33	147.33	23.99	25.4
SP40	58.95	118.67	147	22.52	23.7

Further from the thermograms of PLA and its composites, the mass loss drops significantly starting from the temperature range of about 260 to 300 °C, which may be attributed to the degradation of the material constituents. However, at higher temperatures, the structure of interactions between surfaces and the presence of components such as α -cellulose and lignin in the sansveria fibre may provide heat resistance. The fluctuation of these parameters in the composite is directly proportional to the wt% of sansveria fibres reinforced [47]. As a result, the SP 40 suffered the least weight loss throughout the last stage of degradation. The weight percentage of char residue at 390 °C for PLA composites increased with the increase in SCFP content. This increase in the emergence of the char residue can be affirmed as an improved heat resistance exerted by SCFP. A similar kind of trend was also previously reported by researchers [35].

3.4. Differential scanning calorimetry (DSC)

The degree of crystallinity X_c (%) was estimated from the equation (2) shown below:

$$X_c(\%) = \frac{\Delta H_f}{\Delta H_f^0} \times \frac{100}{w} \quad (2)$$

Where ΔH_f is the melting enthalpy (J/g) for the composite and H_f^0 is the melting enthalpy for 100% crystalline PLA and w is the weight fraction polymer.

Figure 6 presents the DSC thermogram of the SCFP with respect to their fibre loading. T_g , T_{cc} , T_m and degree of crystallinity obtained from the DSC thermogram has been tabulated in table 11. The infinitesimally small difference could be noticed in terms of T_g , T_{cc} , and T_m values for the composites reinforced with various fibre loading. However, neat PLA was found to have slightly higher values than the composites. On the other hand, reinforcing SCF into the PLA matrix promoted the crystallization of PLA by 1%–3% with the maximum degree of crystallinity of 25.4% obtained for the SP30. The increase in the degree of crystallinity and a slight drop in T_g , T_{cc} and T_m with the increase of fibre loading has been consistent with the findings reported in the recent studies with bamboo fibre, wood fibre, and coir fibre-reinforced PLA [48] and pulp fibre/PLA [49]. The higher degree of crystallinity for composites up to 30 wt% is due to the fact that SCF acts as a nucleating agent, which increases the number of nucleation sites, leading to increased transcrystallinity and spherulite growth within the PLA matrix [50].

4. Conclusion

Examining the thermal properties of Short SCFP provided valuable insights into the impact of various fibre loadings. The key conclusions drawn from the results are outlined below.

Reinforcing the SCF into PLA led to a noticeable overall stiffness and rigidity enhancement, as evidenced by the increased E' in the composites. Notably, SP 40 exhibited the highest E across the glass transition and rubbery regions.

At elevated temperatures (>68.5 °C), the SP10 exhibited a significant difference in E'' , retaining higher viscoelastic properties. However, a distinct trend emerged with increased fibre loadings in the PLA matrix.

TGA thermograms revealed a substantial mass loss between 260 °C and 300 °C, indicating that the material constitutes degradation. In terms of weight loss during the final stage of degradation, SP 40 displayed the least weight loss, reporting a residue of 9.01%.

Minimal variations were observed in T_g , T_{cc} , and T_m values among the fabricated samples, with the PLA consistently exhibiting higher values. Introducing SCF into PLA contributed to a 1% to 3% increase in crystallization values, reaching a maximum degree of crystallinity of 25.4% for the SP 30.

Incorporating SCF in PLA positively influenced their thermal characteristics, with varying fibre loadings showcasing distinct effects on stiffness, viscoelasticity, and crystallization behavior. These findings hold significance for tailoring SCFP for specific applications balancing thermal stability.

Acknowledgments

The authors extend their appreciation to the Deanship of Scientific Research at King Khalid University for funding this work through large group Research Project under grant number RGP.2/136/44.

Data availability statement

The data cannot be made publicly available upon publication because no suitable repository exists for hosting data in this field of study. The data that support the findings of this study are available upon reasonable request from the authors.

Conflicts of interest

The authors declare no conflicts of interest.

ORCID iDs

Senthilkumar Krishnasamy  <https://orcid.org/0000-0001-6981-6196>

M Chandrasekar  <https://orcid.org/0000-0002-3637-7630>

T Senthil Muthu Kumar  <https://orcid.org/0000-0003-1443-7222>

Jyotishkumar Parameswaranpillai  <https://orcid.org/0000-0002-3809-8598>

D Aravind  <https://orcid.org/0000-0003-4398-2094>

N Rajini  <https://orcid.org/0000-0002-2337-3470>

Suchart Siengchin  <https://orcid.org/0000-0002-6635-5686>

References

- [1] Peñaloza D, Erlandsson M and Falk A 2016 Exploring the climate impact effects of increased use of bio-based materials in buildings *Constr. Build. Mater.* **125** 219–26
- [2] Andrew J J and Dhakal H N 2022 Sustainable biobased composites for advanced applications: recent trends and future opportunities—a critical review *Composites C* **7** 100220
- [3] Kumar A, Biswal M, Mohanty S and Nayak S K 2021 Recent developments of lignocellulosic natural fiber reinforced hybrid thermosetting composites for high-end structural applications: a review *J. Polym. Res.* **28** 459
- [4] Cruz-Ramos C A 1986 Natural fiber reinforced thermoplastics *Mechanical Properties of Reinforced Thermoplastics* (Springer) 65–81
- [5] Awais H, Nawab Y, Amjad A, Anjang A, Akil H M and Abidin M S Z 2021 Environmental benign natural fibre reinforced thermoplastic composites: a review *Composites C* **4** 100082
- [6] Zhang H, Fan X, Chen W, Wang Y, Liu C, Cui B, Li G, Song J, Zhao D and Wang D 2022 A simple and green strategy for preparing flexible thermoplastic polyimide foams with exceptional mechanical, thermal-insulating properties, and temperature resistance for high-temperature lightweight composite sandwich structures *Composites B* **228** 109405
- [7] Sreenivasan V S, Ravindran D, Manikandan V and Narayanasamy R 2011 Mechanical properties of randomly oriented short *Sansevieria cylindrica* fibre/polyester composites *Mater. Des.* **32** 2444–55

- [8] Sreenivasan V S, Ravindran D, Manikandan V and Narayanasamy R 2012 Influence of fibre treatments on mechanical properties of short *Sansevieria cylindrica*/polyester composites *Mater. Des.* **37** 111–21
- [9] Ashok Kumar M, Hemachandra Reddy K, Ramachandra Reddy G and Vishnu Mahesh KR 2012 Characterization of light weight epoxy composites from short *Sansevieria cylindrica* fibers *Fibers Polym.* **13** 769–74
- [10] Yu M, Huang R, He C, Wu Q and Zhao X 2016 Hybrid composites from wheat straw, inorganic filler, and recycled polypropylene: morphology and mechanical and thermal expansion performance *Int. J. Polym. Sci.* **2016** 1–12
- [11] Zabihzadeh S M 2010 Influence of plastic type and compatibilizer on thermal properties of wheat straw flour/thermoplastic composites *J. Thermoplast. Compos. Mater.* **23** 817–26
- [12] Yang H-S, Gardner D and Kim H-J 2009 Viscoelastic and thermal analysis of lignocellulosic material filled polypropylene bio-composites *J. Therm. Anal. Calorim.* **98** 553–8
- [13] Kismet Y and Dogan A 2022 Characterization of the mechanical and thermal properties of rape short natural-fiber reinforced thermoplastic composites *Iranian Polym. J.* **13** 1–9
- [14] Noor Azammi A M, Sapuan SM, Ishak M R and Sultan M T H 2018 Mechanical and thermal properties of kenaf reinforced thermoplastic polyurethane (TPU)-natural rubber (NR) composites *Fibers Polym.* **19** 446–51
- [15] Jumaidin R, Whang L Y, Ilyas R A, Hazrati K Z, Hafila K Z, Jamal T and Alia R A 2023 Effect of durian peel fiber on thermal, mechanical, and biodegradation characteristics of thermoplastic cassava starch composites *Int. J. Biol. Macromol.* **250** 126295
- [16] Li M, Jia Y, Shen X, Shen T, Tan Z, Zhuang W, Zhao G, Zhu C and Ying H 2021 Investigation into lignin modified PBAT/thermoplastic starch composites: thermal, mechanical, rheological and water absorption properties *Ind. Crops Prod.* **171** 113916
- [17] Hafila K Z, Jumaidin R, Ilyas R A, Selamat M Z and Yusof F A M 2022 Effect of palm wax on the mechanical, thermal, and moisture absorption properties of thermoplastic cassava starch composites *Int. J. Biol. Macromol.* **194** 851–60
- [18] Sreenivasan V S, Somasundaram S, Ravindran D, Manikandan V and Narayanasamy R 2011 Microstructural, physico-chemical and mechanical characterisation of *Sansevieria cylindrica* fibres—An exploratory investigation *Mater. Des.* **32** 453–61
- [19] Prakash K B, Fageehi Y A, Saminathan R, Manoj Kumar P, Saravanakumar S, Subbiah R, Arulmurugan B and Rajkumar S 2021 Influence of fiber volume and fiber length on thermal and flexural properties of a hybrid natural polymer composite prepared with banana stem, pineapple leaf, and S-glass *Adv. Mater. Sci. Eng.* **2021** 1–11
- [20] Tajvidi M, Falk R H and Hermanson J C 2006 Effect of natural fibers on thermal and mechanical properties of natural fiber polypropylene composites studied by dynamic mechanical analysis *J. Appl. Polym. Sci.* **101** 4341–9
- [21] Panaitescu D M, Fierascu R C, Gabor A R and Nicolae C A 2020 Effect of hemp fiber length on the mechanical and thermal properties of polypropylene/SEBS/hemp fiber composites *Journal of Materials Research and Technology* **9** 10768–81
- [22] Tajvidi M and Takemura A 2009 Effect of fiber content and type, compatibilizer, and heating rate on thermogravimetric properties of natural fiber high density polyethylene composites *Polym. Compos.* **30** 1226–33
- [23] Delli E, Giliopoulos D, Bikiaris D N and Chrissafis K 2021 Fibre length and loading impact on the properties of glass fibre reinforced polypropylene random composites *Compos. Struct.* **263** 113678
- [24] Anon Standard Test Method for Plastics: Dynamic Mechanical Properties: In Flexure (Dual Cantilever Beam) 1
- [25] Anon Standard Test Method for Linear Thermal Expansion of Solid Materials by Thermomechanical Analysis 1
- [26] Anon Standard Test Method for Compositional Analysis by Thermogravimetry 1
- [27] Anon Standard Test Method for Transition Temperatures and Enthalpies of Fusion and Crystallization of Polymers by Differential Scanning Calorimetry 1
- [28] Saba N, Jawaid M, Alothman O Y and Paridah M T 2016 A review on dynamic mechanical properties of natural fibre reinforced polymer composites *Constr. Build. Mater.* **106** 149–59
- [29] Krishnasamy S, Thiagamani S M K, Kumar C M, Nagarajan R, Shahroze R M, Siengchin S, Ismail S O and MP I D 2019 Recent advances in thermal properties of hybrid cellulosic fiber reinforced polymer composites *Int. J. Biol. Macromol.* **141** 1–13
- [30] Huda M S, Drzal L T, Mohanty A K and Misra M 2006 Chopped glass and recycled newspaper as reinforcement fibers in injection molded poly (lactic acid)(PLA) composites: a comparative study *Compos. Sci. Technol.* **66** 1813–24
- [31] Cristea M, Ionita D and Iftime M M 2020 Dynamic mechanical analysis investigations of PLA-based renewable materials: how are they useful? *Materials* **13** 5302
- [32] Greco A and Ferrari F 2021 Thermal behavior of PLA plasticized by commercial and cardanol-derived plasticizers and the effect on the mechanical properties *J. Therm. Anal. Calorim.* **146** 131–41
- [33] Qiao J, Zhang Q, Wu C, Wu G and Li L 2022 Effects of fiber volume fraction and length on the mechanical properties of milled glass fiber/polyurea composites *Polymers* **14** 3080
- [34] Menard K P and Menard N 2020 *Dynamic Mechanical Analysis* (CRC Press)
- [35] Sreenivasan V S, Rajini N, Alavudeen A and Arumugaprabu V 2015 Dynamic mechanical and thermo-gravimetric analysis of *Sansevieria cylindrica*/polyester composite: effect of fiber length, fiber loading and chemical treatment *Composites B* **69** 76–86
- [36] Righetti M C, Cinelli P, Mallegni N, Massa C A, Bronco S, Stähler A and Lazzeri A 2019 Thermal, mechanical, and rheological properties of biocomposites made of poly (lactic acid) and potato pulp powder *Int. J. Mol. Sci.* **20** 675
- [37] Oksman K, Skrifvars M and Selin J-F 2003 Natural fibres as reinforcement in polylactic acid (PLA) composites *Compos. Sci. Technol.* **63** 1317–24
- [38] Pothan L A, Oommen Z and Thomas S 2003 Dynamic mechanical analysis of banana fiber reinforced polyester composites *Compos. Sci. Technol.* **63** 283–93
- [39] Indira K N, Jyotishkumar P and Thomas S 2014 Viscoelastic behaviour of untreated and chemically treated banana Fiber/PF composites *Fibers Polym.* **15** 91–100
- [40] Choi H Y and Lee J S 2012 Effects of surface treatment of ramie fibers in a ramie/poly (lactic acid) composite *Fibers Polym.* **13** 217–23
- [41] Jin F-L, Hu R-R and Park S-J 2019 Improvement of thermal behaviors of biodegradable poly (lactic acid) polymer: a review *Composites B* **164** 287–96
- [42] Neto J S S, de Queiroz H F M, Aguiar R A A and Banea M D 2021 A review on the thermal characterisation of natural and hybrid fiber composites *Polymers* **13** 4425
- [43] Schawe J E K and Ziegelmeier S 2016 Determination of the thermal short time stability of polymers by fast scanning calorimetry *Thermochim. Acta* **623** 80–5
- [44] Krishnasamy S, Thiagamani S M K, Muthu Kumar C, Nagarajan R, Shahroze R M, Siengchin S, Ismail S O and Indira I D 2019 Recent advances in thermal properties of hybrid cellulosic fiber reinforced polymer composites *Int. J. Biol. Macromol.* **141** 1–13
- [45] Krishnasamy S, Thiagamani S M K, Muthukumar C, Tengsuthiwat J, Nagarajan R, Siengchin S and Ismail S O 2019 Effects of stacking sequences on static, dynamic mechanical and thermal properties of completely biodegradable green epoxy hybrid composites *Mater. Res. Express* **6** 105351

- [46] Krishnasamy S, Thiagamani S M K, Muthukumar C, Nagarajan R and Siengchin S 2021 *Natural Fiber-Reinforced Composites: Thermal Properties and Applications* (Wiley)
- [47] Sathishkumar T P, Navaneethakrishnan P, Shankar S and Rajasekar R 2013 Characterization of new cellulose sansevieria ehrenbergii fibers for polymer composites *Compos. Interfaces* **20** 575–93
- [48] Zhang Q, Shi L, Nie J, Wang H and Yang D 2012 Study on poly (lactic acid)/natural fibers composites *J. Appl. Polym. Sci.* **125** E526–33
- [49] Du Y, Wu T, Yan N, Kortschot M T and Farnood R 2014 Fabrication and characterization of fully biodegradable natural fiber-reinforced poly (lactic acid) composites *Composites B* **56** 717–23
- [50] Sawpan M A, Pickering K L and Fernyhough A 2007 Hemp fibre reinforced poly (lactic acid) composites *Adv. Mat. Res.* **29** 337–40